Tight temporal coupling between synaptic rewiring of olfactory glomeruli and the emergence of odor-guided behavior in *Xenopus* tadpoles

Beatrice Terni[1,2], Paolo Pacciolla[1,2], Helena Masanas[2,4], Pau Gorostiza[4,5] and Artur Llobet[1,2,3,*]

[1] Laboratory of Neurobiology, Department of Pathology and Experimental Therapeutics, Faculty of Medicine, University of Barcelona, 08907 L'Hospitalet de Llobregat, Barcelona, Spain

[2] Bellvitge Biomedical Research Institute (IDIBELL), 08907 L'Hospitalet de Llobregat, Barcelona, Spain

[3] Institute of Neurosciences, University of Barcelona, 08907 L'Hospitalet de Llobregat, Barcelona, Spain

[4] Institut de Bioenginyeria de Catalunya (IBEC), Barcelona 08028, Spain.

[5] Institució Catalana de Recerca i Estudis Avançats (ICREA), Barcelona 08010, Spain.

* Corresponding author:
Laboratory of Neurobiology
Faculty of Medicine - University of Barcelona
Bellvitge Biomedical Research Institute (IDIBELL)
08907 L'Hospitalet de Llobregat
Barcelona, Spain
e-mail: allobet@ub.edu
Phone: +34-934024279
Fax: +34-934035810

Olfactory sensory neurons (OSNs) are chemoreceptors that establish excitatory synapses within glomeruli of the olfactory bulb. OSNs undergo continuous turnover throughout life, causing the constant replacement of their synaptic contacts. Using *Xenopus* tadpoles as an experimental system to investigate rewiring of glomerular connectivity, we show that novel OSN synapses can transfer information immediately after formation, mediating an olfactory-guided behavior. Tadpoles recover the ability to detect amino acids four days after bilateral olfactory nerve transection. The restoration of olfactory-guided behavior depends on the efficient reinsertion of OSNs to the olfactory bulb. Presynaptic terminals of incipient synaptic contacts generate calcium transients in response to odors, triggering long lasting depolarization of olfactory glomeruli. The functionality of reconnected terminals relies on well-defined readily releasable and cytoplasmic vesicle pools. The continuous growth of non-compartmentalized axonal processes provides a vesicle reservoir to nascent release sites, which contrasts to the gradual development of cytoplasmic vesicle pools in conventional excitatory synapses. The immediate availability of fully functional synapses upon formation supports an age-independent contribution of OSNs to the generation of odor maps.

Keywords: olfactory receptor neurons; olfactory bulb; presynaptic terminals; synaptic vesicles; RRID:SCR_013731; RRID:SCR_007164; RRID: AB-887824; RRID: AB-221570

Abreviations:

OSN: Olfactory Sensory Neuron

INTRODUCTION

Olfactory sensory neurons (OSNs) are distributed throughout the olfactory epithelium to transduce chemical information carried by odorants. OSNs send their axons to the olfactory bulb and transmit information to mitral and tufted (M/T) cells via glutamatergic synapses located within glomeruli (G.M. Shepherd, Chen, & Greer, 2004). Turnover is a unique feature of OSNs, since they have a life span of 30 to 120 days and are constantly replenished from basal cells of the olfactory epithelium (Cheetham, Park, & Belluscio, 2016; Mombaerts, 2006). Since each glomerulus receives inputs from a single population of OSNs expressing a given olfactory receptor, the axons from newborn OSNs must find their correct target in order to maintain processing of odor information. The targeting of olfactory glomeruli by OSNs is highly specific (Treloar, Feinstein, Mombaerts, & Greer, 2002): during development axonal branching only occurs upon entering a glomerulus and is rarely observed in the nerve layer (Klenoff & Greer, 1998). This well-established ability of newborn neurons to continuously rewire odor maps contrasts with the gap of knowledge regarding how new synapses intermingle with pre-existing glomerular connectivity and become involved in the processing of olfactory information (Zou, Chesler, & Firestein, 2009).

The assembly of excitatory synapses takes place in a stereotyped manner within a time window of minutes. Vesicles containing presynaptic cytomatrix proteins are transferred to axon terminals to form functional active zones while glutamate receptors are gradually inserted in the postsynaptic density. As a result, recently formed synapses acquire capacity for evoked exo and endocytosis in less than 45 min (Friedman, Bresler, Garner, & Ziv, 2000) but are not fully functional. To achieve this aim synapses require a maturation process that lasts several weeks (Waites, Craig, & Garner, 2005), characterized by: an increase in pre and postsynaptic terminal size, the development of synaptic vesicle pools and a decrease in release probability (Mozhayeva, Sara, Liu, & Kavalali, 2002). Noticeably, only a fraction of established contacts are selected for

maturation since multiple embryonic synapses are pruned. All of these pieces of evidence, mostly gathered from synapses established on spines, illustrate the information processing requirements of higher brain areas during development, however, it is still unknown whether they are applicable to the continuous synaptic turnover of olfactory glomeruli.

The lack of data supporting selective pruning of axonal branches within glomeruli suggests that most of synaptic contacts established by newly formed OSNs undergo maturation (Klenoff & Greer, 1998). As a result, two possible scenarios can be drawn. If, similarly to other glutamaergic synapses, established contacts require weeks for completing their maturation, the contribution of individual OSNs to glomerular excitation should be age-dependent. Older neurons would thus provide qualitatively different responses to younger neurons due to the presence of a larger number of fully functional synapses. In contrast, if maturation were accomplished faster than conventional excitatory synapses, newly formed contacts would be virtually equivalent to consolidated contacts. In this scenario, the difference among young and old OSNs projecting to a given glomerulus should essentially reside on the number of synapses established.

To address this question we took advantage of the well-described capacity of *Xenopus* tadpoles to rewire their olfactory connectivity after injury (Stout & Graziadei, 1980; Yoshino & Tochinai, 2006). Olfactory nerve transection caused the complete loss of glomeruli. We observed that OSN axons require days to consolidate an extensive network of glomerular connectivity but surprisingly, newly formed synapses displayed numerous synaptic vesicles throughout the process of glomerular reformation, mediated long lasting depolarizations upon exposure to waterborne odorants and supported odor-guided behavioral responses, altogether suggesting the acquisition of the ability to process information rapidly after formation. In the light of our results, the age of OSNs essentially determines the number but not the functional properties of established intraglomerular synapses.

METHODS

Animals

Ethical procedures were approved by the regional government (Generalitat de Catalunya, experimental procedure #9275). *X. tropicalis* and *X. laevis* tadpoles were housed and raised according to standard methods. Larvae were obtained by either natural mating or in vitro fertilization of adult animals and kept in tanks at 25 °C. Water conductivity was adjusted to ~700 μS, pH 7.5 and ~1400 μS, pH 7.8 for *X. tropicalis* and *X. laevis* tadpoles, respectively. Tadpoles at stages 48-52 of the Nieuwkoop–Faber criteria were used for the experiments. To visualize the time-course of olfactory nerve reformation we took advantage of two transgenic lines expressing GFP under a neuronal β-tubulin promoter: *X. laevis* tubb2b-GFP and *X. tropicalis* NBT-GFP. Both lines allow the visualization of the entire nervous system and particularly of olfactory nerves. The transgenic *X. tropicalis* line zHB9-GFP, generated from the zebrafish HB9 gene (Flanagan-Steet, Fox, Meyer, & Sanes, 2005) allowed visualization of discrete glomerular structures. Although HB9 is a transcription factor specific of motor neurons it drives the ectopic expression of GFP in a subset of OSNs, as reported in mice (Nakano, Windrem, Zappavigna, & Goldman, 2005). The transgenic *X. laevis* line tubb2-GFP was obtained from the National *Xenopus* Resource (NXR, Woods Hole, MA, RRID:SCR_013731). Transgenic *X. tropicalis* lines NBT-GFP and zHB9-GFP were established from frozen sperm obtained from the European *Xenopus* Resource Centre (EXRC, Portsmouth, UK, RRID:SCR_007164). Unilateral and bilateral sectioning of olfactory nerves were performed using 8 cm scissors (WPI, cat # 501778) in tadpoles anesthetized in 0.02% MS-222. Efficient olfactory nerve transection was certified by visual inspection. Line profiles were also drawn along sectioned nerves labeled with DiI-CM

(C7001, Molecular Probes) to verify cuts. Tadpoles were observed under a stereomicroscope to follow nerve reformation.

Assay of olfactory-guided behavior

The assay of an olfactory-guided response was performed using free swimming *X. tropicalis* tadpoles in a six-well dish placed on a custom made LED transilluminator. Each well contained 10 mL of tadpole water and a single animal. Tadpoles rested during 3-5 minutes before performing behavioral analysis. Individual perfusion inlets allowed the delivery of waterborne odorants, which consisted in a mixture of five different amino acids (methionine, leucine, histidine, arginine and lysine) that acted as a broad-range stimulus of OSNs (Manzini, Brase, Chen, & Schild, 2007). Stock solutions (10 mM) of each amino acid were prepared in Xenopus Ringer, which contained (in mM):100 NaCl, 2 KCl, 1 $CaCl_2$, 2 $MgCl_2$, 10 glucose, 10 HEPES, 240 mOsm/kg, pH=7.8. The final 160 μM amino acid mixture was prepared in Xenopus water in a final volume of 20 mL, pH =7.2. The solution was kept in an elevated reservoir, connected to a six-line manifold using propylene tubing. Upon opening a clamp, 3.3 mL of the solution were added within ~35 s to each dish well. This maneuver created a localized source of waterborne odorants. Delivery of a 160 μM fast green (Sigma-Aldrich, St. Louis, MO) solution showed that dye dispersal within the well became homogeneous ~5s after perfusion onset, thus defining this time interval as a maximum latency to obtain a behavioral response. To evaluate possible mechanosensitive effects generated by the flow of incoming solution, controls were established by substituting MQ water for the amino acid solution. Tadpole movements were not restricted, considering their average length was ~12 mm, about 1/3 the size of the well diameter (35 mm). Swimming was continuously recorded using a digital camera (Olympus) or an MRC5 camera (Zeiss). Movies were imported in Image J, decimated to 6 Hz and analyzed with the MTrackJ and Wrmtrck plugins (Meijering, Dzyubachyk, & Smal, 2012; Nussbaum-Krammer,

Neto, Brielmann, Pedersen, & Morimoto, 2015). Individual tracks were exported to Igor Pro software 7.0 for calculating the euclidean distance to the odorant source.

Histological procedures

Tadpoles were fixed for immunohistochemistry during 2-7 days in 4% PFA and immersed in sucrose. Animals were next embedded in O.C.T. freezing medium (Tissue-Tek®, Sakura Finetek, Zoeterwoude, the Netherlands), snap-frozen in isopentane in a Bright Clini-RF rapid freezer and stored at –80 °C until use. Coronal sections (15-30 μm thick) were obtained using a cryostat (Leica, Reichert-Jung, Heidelberg, Germany) and mounted on superfrost plus slides (VWR Scientific). Sections were blocked for 2 h with PBS solution containing 0.2% Triton X-100 and 10% NGS, and next incubated in a moist chamber overnight at 4 °C in PBS with 0.2% Triton X-100 and 2% NGS containing anti-synaptophysin (mouse monoclonal, Synaptic Systems 101011, 1:200, RRID: AB-887824) and anti-GFP (rabbit polyclonal, A6455, Invitrogen, 1:300, RRID: AB-221570). After three washes with PBS, sections were incubated with appropriate secondary antibodies and mounted in mowiol.

For electron microscopy tadpoles were fixed in a 1.5% glutaraldehyde solution prepared in PB, adjusted to ~300 mOsm/kg, pH=7.8. To visualize DiI labeled processes, photoconversion was carried out after fixation following previously described methods (Singleton & Casagrande, 1996). Tadpoles were postfixed in 1% osmium tetroxide/1.5% potassium ferricyanide, dehydrated, and embedded in epon. Upon identification of the glomerular region, ultrathin sections (60 nm) were stained with uranyl acetate and lead citrate and viewed under a JEOL 1010 electron microscope.

Antibody characterization

Primary antibody details are shown in Table 1. The rabbit anti-GFP antibody specificity was verified for immunohistochemistry by the manufacturer and further details for its validation

158 are described elsewhere (Haws et al., 2014). In our study the GFP staining was observed only in
159 the nervous system where the expression of the GFP was regulated by the specific promoters
160 neural beta tubulin (Marsh-Armstrong, Huang, Berry, & Brown, 1999) or zHB9 (Arber et al.,
161 1999). The specificity of mouse anti synapthophysin 1 was verified by western-blot by the
162 manufacturer. The labeling of glomerular structures in the olfactory bulb perfectly matched
163 glomeruli stained by DiI injected at the level of the olfactory placodes.
164
165 **In vivo measurement of synaptic activity**
166 *X. tropicalis* tadpoles were anesthetized in 0.02% MS-222 and placed on wet paper.
167 Olfactory placodes were injected with 0.15-0.3 µL of a solution containing 12% Calcium Green-
168 1-dextran (10 kDa; Molecular Probes, Eugene, OR), 0.1% Triton X-100, and 1 mM NaCl
169 (Friedrich & Korsching, 1997). Dye was washed out during 2–4 min and tadpoles returned to
170 tanks. Two to three days after injection the glomerular layer of the olfactory bulb showed a
171 homogenous fluorescence. To measure evoked olfactory responses, tadpoles were anesthetized
172 with 0.02% MS-222 and the portion of skin covering the olfactory bulb was removed. Animals
173 were next placed in a well fabricated in a sylgard-coated dish. A coverslip restricted tadpole
174 movements and leaved olfactory placodes and bulbs accessible. Animals were transferred to the
175 stage of an upright microscope (Zeiss, Axioexaminer A1) and continuously perfused with
176 Xenopus Ringer (see composition above), supplemented with 100 µM d-tubocurarine to prevent
177 muscle contractions.
178 Olfactory bulbs were viewed with a 63x/0.9 N.A water immersion objective (Figs 8A and
179 B). Images (250x250 pixels) were acquired with an Image EM camera at 33 Hz. A TTL signal
180 delivered by a Master-8 stimulator (AMPI, Israel) commanded the opening of a solenoid valve
181 during 0.5 s to locally apply a 200 µM solution of methionine, leucine, histidine, arginine and
182 lysine prepared in Xenopus Ringer. The solution was delivered through a 28 G microfil needle
183 (WPI, Sarasota, FL) on the top of a single olfactory placode. Movies were imported in Image J

and ΔF/F changes in fluorescence were measured as $((F-F_0)/F_0)\cdot 100$. Glomerular structures showing calcium responses upon amino acid exposure were selected by defining regions of interest (ROIs). The mean calcium transient evoked in the presynaptic terminal of OSNs was calculated by averaging the response of individual ROIs using Igor Pro 7.0.

For electrophysiology tadpoles were placed in sylgard-coated dishes using the same procedure and solutions applied for imaging experiments. A 10x objective was used to locate olfactory pathways and to place the recording electrode in the glomerular layer. Pipettes had a ~2 MΩ resistance and were filled with extracellular solution. As for imaging experiments, a Master-8 stimulator (AMPI, Israel) commanded the delivery during 0.1 s of a 200 μM solution of methionine, leucine, histidine, arginine and lysine on the top of a single olfactory placode. Recordings of local field potentials were made using an Axopatch 200B controlled by WCP software (Dr. John Dempster, University of Strathclyde). Signals were acquired at 10 KHz, low pass filtered offline <100 Hz and analyzed with Igor Pro 7.0.

Statistical analysis

For statistical analysis, the unpaired Student's t test was used to evaluate differences between two experimental groups. Comparisons among three or more groups were performed using one-way ANOVA, followed by the Bonferroni post hoc test.

RESULTS

Xenopus tadpoles recover odor-guided behavior within four days after olfactory nerve transection

The olfactory system of *Xenopus* tadpoles shows an exquisite sensitivity to detect amino acids in water, which effectively behave as waterborne odorants (Hassenklöver, Pallesen, Schild, & Manzini, 2012). Through at least 36 classes of ORNs, *Xenopus* larvae elaborate a map of odors by activating specific glomeruli projecting to M/T cells (Manzini & Schild, 2004). The exposure of *X. tropicalis* tadpoles to a mixture of 5 amino acids (methionine, leucine, histidine, arginine, lysine), aiming to stimulate a broad range of glomeruli (Manzini, Brase, et al., 2007), evoked an olfactory-guided behavior. The odorant solution was applied to tadpole water using a custom-made perfusion system at ~0.9 $mmol \cdot cm^{2} \cdot s^{-1}$ through inlets fabricated on a 6-well dish (Fig 1a). When animals noticed the arrival of odorants, they moved towards the incoming solution and transiently inspected the region enriched in amino acids. Consequently, the euclidean distance between the odorant source and the tadpole head was minimal during the application of the odorant solution (Fig.1b).

The odor-guided motor response was used to estimate the time required by OSNs to achieve functional insertion in olfactory bulb circuitry. The recovery of the ability to sense waterborne odorants was evaluated after sectioning both olfactory nerves. Transection of olfactory nerves is a well-established method to induce death of OSNs and to promote neurogenesis in the olfactory epithelium (Doucette, Kiernan, & Flumerfelt, 1983). Under these experimental conditions the olfactory bulb circuitry and placode neuronal precursor cells remain intact. The damage is exclusively targeted to OSNs, thus forcing their synchronous replenishment by newborn neurons. Tadpoles did not respond to the presence of amino acids one day after injury (D1, Fig.1c), however, the characteristic odor-guided behavior was again obvious four days after surgery (D4, Fig.1d). Corresponding control experiments substituting amino acids by water excluded the participation of non-odorant mechanisms (Fig. 2a). Tadpoles moved randomly before, during and after the inflow of water, which contrasted to the olfactory-guided behavior caused by the arrival of the amino acid solution. On average, control tadpoles responded with a linear approximation to the odor source at 0.57 $mm \cdot s^{-1}$ (r^{2}=0.94), reaching a minimum ~20 s after

perfusion onset (Fig. 2b). This characteristic behavior was not observed one day after transection (D1, Fig. 2c) but emerged 4 days after surgery (D4, Fig. 2d). Tadpoles showed a linear approximation to the odor source (0.43 $mm \cdot s^{-1}$, r^2=0.94), reaching again a minimum ~20 s after perfusion onset. Averaged data confirmed that within four days tadpoles recover an odor-guided behavior associated to the establishment of functional synapses among OSN axons and pre-existing olfactory bulb circuitry, thus defining a temporal window for the effective insertion of newborn neurons in a neuronal network.

Xenopus tadpoles efficiently reform olfactory nerves after injury

The exquisite labeling of olfactory nerves in *X. laevis* tubb2b-GFP and *X. tropicalis* NBT-GFP tadpoles allowed cutting a single olfactory nerve leaving intact the contralateral one, which acted as control (Fig. 3a). The damaged nerve disappeared one day after transection, likely reflecting the death of OSNs. The complete absence of olfactory nerve input to the olfactory bulb was verified by DiI staining (Figs. 3b and c). Reformation was on average successful in ~85% of the animals and occurred in two phases: reconnection and thickening (Fig. 3d). Reconnection to the olfactory bulb was evident three to four days after injury, followed by an exponential increase in nerve thickness that occurred with a time constant of 17 h and 19 h for *X. tropicalis* and *X. laevis*, respectively (Fig. 3e). Reformed nerves were however, always thinner than corresponding controls.

These experiments revealed that the capacity of the *Xenopus* olfactory system to recover from injury is about an order of magnitude faster than rodents (Herzog & Otto, 2002). Formation of finer nerves (Figs. 3e) suggested that newborn OSNs did not completely compensate losses induced by damage. Considering the nerve as a cylindrical structure and an unaffected ensheathing by glial cells, the described ~20% reduction in nerve width should be associated to a ~36% decrease in volume. Therefore, a comparable lower number of OSNs should be expected

in the placode. These figures could account for the recovery of olfactory guided behavior (Figs. 1 and 2) taking into account the high degree of redundancy of the olfactory system (Lu & Slotnick, 1998). The next step was investigating how synaptic connectivity was arranged to allow the emergence of olfactory-guided behavior ~48h after the arrival of OSN axons to the olfactory bulb.

Olfactory information can be conveyed by immature glomerular structures

Xenopus tadpoles contain about 300 distinct glomeruli (Manzini, Heermann, et al., 2007; Nezlin & Schild, 2000), receiving information from OSNs whose cell bodies are located in the main cavity and detect waterborne odorants (Gaudin & Gascuel, 2005). Although individual glomeruli have a unique contribution to the elaboration of odor maps according to the expression of olfactory receptors (Manzini & Schild, 2004), they show comparable synaptic properties. The homogenous expression of the synaptic markers syntaxin, SNAP25 and synaptophysin suggests a similar density of synaptic contacts among the glomerular layer (Manzini, Heermann, et al., 2007). Synaptophysin staining of tubb2b-GFP st. 49-52 *X. laevis* tadpoles revealed the presence of numerous glomeruli (Figs. 4a and b) with a mean perimeter of 64±1 μm (n=179). Only ventral sections showing the arrival of the olfactory nerve were considered. The dorsal portion of the olfactory bulb was excluded from analysis, since this region lacks well-defined glomerular structures (Gaudin & Gascuel, 2005; Manzini, Heermann, et al., 2007; Nezlin & Schild, 2000).

Sectioning of the olfactory nerve caused profound changes in the glomerular layer (Figs. 4a and b). Up to one week after injury synaptophysin staining did not reveal the reformation of glomerular structures. It was 8 days from transection when numerous synaptophysin positive puncta formed clusters in the ipsilateral bulb to the injured nerve and small, well-defined glomerular structures were obvious (Fig. 4a). As tadpole development proceeded, the number of glomeruli was lower in the rewired than in the control bulb, but on average, the size of reformed glomerular structures reached control values ~15 days after injury (Figs. 4b, c). These results

showed that de novo formation of mature glomerular units required weeks, hence basic olfactory-guided behavior (Figs. 1 and 2) was likely mediated by simpler connectivity.

Visualization of synaptophysin staining provided readout of the time required for the overall reformation of glomeruli, however, the widespread labeling made not it possible to compare specific glomerular structures between control and rewired bulbs. Living zHB9-GFP tadpoles embedded in agarose showed motor neurons labeled with GFP and, similarly to mice, also displayed discrete labeling of olfactory glomeruli. Fluorescent OSNs sent their axons to the olfactory bulb and projected to three distinct glomerular units (GUs, Figs. 4d and e), which we termed lateral (L), medial-1 (M1) and medial-2 (M2). All tadpoles inspected (n=52) showed the L-GU, which appeared alone or in combination with M1 and/or M2 GUs. The M2-GU was the smallest. Its size and location suggested a relationship to β or γ glomeruli, while L-GU and M1-GU were integrated within the lateral and intermediate glomerular clusters described elsewhere (Gaudin & Gascuel, 2005; Manzini, Heermann, et al., 2007).

The characteristic glomerular pattern present in zHB9-GFP tadpoles was used to follow the rewiring of specific GUs. In agreement with synaptophysin stainings (Figs. 4a and b), we did not observe the formation of glomeruli 4 to 10 days after injury, however, localized fluorescence spots appeared in 23% of animals studied (n=40) in the region corresponding to L, M1 or M2 GUs (Fig. 4e). The absence of aberrantly located GUs supported a correct targeting of postsynaptic partners by newly formed OSNs. Considering the spatial resolution of our in vivo approach (~1 μm) limited the discrimination of axonal processes, we visualized GFP expression by immunohistochemistry in histological sections. As expected, the axonal tuft of OSNs in control bulbs showed branches adopting a characteristic spherical organization (Fig. 4f). Although the processes rewiring lost connectivity did show branch formation, lacked a glomerular-like appearance (Fig. 4g). These results are consistent with the recovery of olfactory-driven behavior 4 days after injury (Figs. 1 and 2) and could be attributed to the reformation of a viable connectivity that was not yet establishing a complex presynaptic glomerular network.

The analysis of olfactory placodes in zHB9-GFP tadpoles revealed a five-fold reduction in the number of cell bodies caused by nerve transection, thus supporting reformation of finer olfactory nerves was caused by a decrease in OSNs (see also Figs. 3d and e). In terms of the whole glomerular tuft, glomerular volume was linearly related to the number of cell bodies identified in the ipsilateral placode (Fig. 4h) as previously reported (Bressel, Khan, & Mombaerts, 2016). The average contribution of a single axonal arbor was 874 μm^3, which is within the range of the previously reported value of 1077 μm^3 for *X. laevis* tadpoles (Hassenklöver & Manzini, 2013). This observation supports that labeled glomeruli in zHB9 larvae could be considered as representative individual examples of the glomerular layer.

Glomerular tufts contain a constant density of cytoplasmic vesicles throughout development

The discrete enlargements of axonal arbors visualized in GFP labeled glomeruli (Figs. 4f and g) are presumably associated to the establishment synapses (Hassenklöver & Manzini, 2013), suggesting synaptic contacts were formed immediately after OSN axons entered to the olfactory bulb. To resolve how incipient synapses were integrated with pre-existing olfactory bulb circuitry we compared the ultrastructure of control and rewired presynaptic terminals using *X. tropicalis* tadpoles with both olfactory nerves sectioned. Low magnification electron micrographs revealed discrete glomerular structures (Fig.5a) that were separated from the nerve layer by juxtaglomerular neurons, as previously reported (Nezlin, Heermann, Schild, & Rössler, 2003). The terminals of OSN axons, which were identified by their dark cytoplasmic staining (Hinds & Hinds, 1976; G. M. Shepherd, 1972), formed an intricate network that gave rise to glomeruli by projecting on dendrites presumably from M/T cells. The separation among glomerular structures was not always obvious, due to the lack of surrounding astrocytes (Nezlin et al., 2003). Axodendritic synapses (Figs. 5b and c) were enriched within discrete glomerular regions thus suggesting their compartimentalization, similarly to the mammalian olfactory bulb (Kasowski, Kim, & Greer, 1999). In agreement with optical microscopy (Fig. 4), such characteristic

organization was not observed in rewired bulbs 4 and 6 days after injury. Groups of axons entered to the bulb and their tips started to converge on dendrites, giving rise to structures that could be interpreted as precursors of glomeruli (Figs. 5d-i). Although well-defined glomerular structures were not detected, there were obvious signs of functional connectivity between OSNs and dendrites, illustrated by the emergence of pre and postsynaptic densities. Precursors of glomerular structures continued increasing their size and complexity as a function of time, until the establishment of well-defined glomeruli 15 days after olfactory nerve transection. At this stage, glomerular structure and connectivity was comparable to control bulbs (Figs. 5j-l).

Prominent active zones, as well as a high synaptic vesicle density found in the tortuous axonal processes of control tadpoles (Figs. 5b and c), guarantee an efficient neurotransmitter release in intraglomerular synapses (Doucette et al., 1983; Kasowski et al., 1999; G.M. Shepherd et al., 2004). Active zones in control tadpoles showed a mean length of 321±12 nm (n=37, 3 animals) and on average attached 11±1 vesicles (Fig. 6a). Synaptic vesicles homogenously filled the entire surface of the cytoplasm at 112±7 vesicles·μm^{-2} (n=30, Fig. 6b). The proportion between synaptic vesicles found in the cytoplasm and those attached to active zones was maintained constant throughout glomerular reformation (Figs. 6a and b). The distribution of synaptic vesicles throughout the cytoplasm remained stable, being found 127±18 vesicles·μm^{-2} (n=14) and 131±13 vesicles·μm^{-2} (n=22) in D4 and D6 animals, respectively. In terms of active zone length, although there was a transient reduction in D4 tadpoles ($p<0.01$), the number of vesicles attached to release sites was again constant during the rewiring process (Figs. 6a). Considering the implication of anterograde transport in vesicle formation (Rizzoli, 2014), the extensive network of microtubules present in axonal processes of OSNs in the early stages of rewiring (Figs. 5e and i) probably played a key role in the coordinated development of axonal arbors and vesicle pools.

Effect of postsynaptic environment on the rewiring of olfactory glomeruli

In about 15% of tadpoles inspected an aberrant nerve reformed, failing to re-establish a connection with the olfactory bulb (Fig. 3e). When present, the new nerve emanated from the placode, travelled caudally paralleling the route of trigeminal nerve and ended by connecting with the hindbrain. The rerouted nerve was thinner than the contralateral olfactory nerve. It was revealed in transgenic tadpoles (*X. laevis* tubb2b-GFP and *X. tropicalis* NBT-GFP) and by DiI stainings obtained by local injection of placodes (Fig. 7a). Surprisingly, the aberrant connection was stable. A given nerve could be observed for more than 10 days (Fig. 7b), suggesting the establishment of permannent connectivity. DiI labelled processes revealed tortuous axons distributed along the rostro-caudal axis at the level of the hindbrain (Fig. 7c) but there was no evidence for the formation of glomeruli.

In order to resolve synapses established at the level of the hindbrain, DiI was photoconverted and the generated precipitate was observed by electron microscopy. The procedure was initially set-up for non-sectioned olfactory nerves. As expected, the procedure revealed the complex network formed by presynaptic axons within a single glomerulus (Figs. 7d-f). OSN axons rerouted to the hindbrain did not converge on dendrites, which contrasted to the characteristic appearance of glomeruli. Axonal processes travelled among dendritic shafts (Fig. 7g), without signs of specific connectivity. Irregularly distributed varicosities containing synaptic vesicles contacted the dendritic tree of hindbrain neurons to form putative synaptic contacts (Figs. 7h and i). All evidences gathered from aberrant synapses showed that the particular postsynaptic environment of the olfactory bulb instructed the ability of OSNs to reform glomerular structures.

Incipient synapses established by olfactory sensory neurons are functional

The presynaptic function of OSNs was evaluated in vivo by visualizing changes in intracellular calcium concentration. Sensory neurons from *X. tropicalis* tadpoles subjected to

388 unilateral sectioning of an olfactory nerve were loaded with calcium green dextran, following
389 methods described for zebrafish (Friedrich & Korsching, 1997). Basal fluorescence in control
390 olfactory bulbs revealed tortuous presynaptic axons (Fig.8a). In contrast, rewired bulbs 4 days
391 after injury showed a distinct pattern. Clusters of fluorescent spots substituted glomerular
392 structures (Fig.8b). Upon 0.5 s exposure of olfactory placodes to a 200 μM solution of five
393 different amino acids (methionine, leucine, histidine, arginine, lysine) a subset of presynaptic
394 terminals responded with transient increases of basal fluorescence (Fig. 8c). Repetition of the
395 procedure in rewired bulbs provided similar responses (Fig. 8d). On average, amino acid
396 application caused a ΔF/F in control tadpoles of 5.7±1 % (n=6). In reinnervated bulbs, calcium
397 transients were comparable, showing a ΔF/F of 7.7±1 % (n=5). Time to peak was also similar
398 being of 0.89±0.2 s and 0.81±0.1s for control and rewired bulbs, respectively (Fig. 8e). These
399 results supported that presynaptic terminals of incipient synaptic contacts formed between OSNs
400 and M/T cells correctly coupled olfactory transduction to calcium dependent release of
401 neurotransmitters.

402 Further information was obtained by recording local field potentials (LFPs) in vivo. Using
403 an electrode placed in the glomerular layer we measured the characteristic long lasting
404 depolarizations triggered by the activation of OSNs (Gire et al., 2012). Stimulation was evoked
405 by 100 ms application of the 200 μM amino acid solution, as previously performed for calcium
406 imaging. Control tadpoles responded to the application of waterborne odorants showing an
407 inward deflection of the LFP (Fig. 9a). Responses were reproducible: stimuli delivered at a time
408 interval of >1 min provided comparable changes of the LFP. Four days after cut, the reinnervated
409 olfactory bulb also displayed the characteristic inward deflection of the LFP upon application of
410 the amino acid mixture (Fig. 9b). As in controls, repetitive stimuli provided comparable
411 responses, showing that olfactory transduction at the placode level was being successfully
412 processed at the level of the olfactory bulb. However, the amplitude of evoked responses in

rewired bulbs was about three fold smaller than controls (Fig. 9c). Since long lasting depolarizations are triggered by OSN stimulation but are amplified by local excitatory interactions among the intraglomerular tufts of M/T cells (Carlson, Shipley, & Keller, 2000), the observed decrease could be attributed, as suggested by morphology experiments, to a lower density of glomerular synapses.

A way to assay the functionality of synaptic contacts established by OSNs was measuring short-term plasticity of long lasting depolarizations. To this aim, the amino acid mixture was delivered by a paired-pulse protocol with time intervals ranging from 2.5 s to 1 min. Control bulbs showed a characteristic recovery from short-term depression, occurring with a time constant of 18 s (Figs. 9d and e). The small responses of rewired bulbs precluded obtaining an accurate paired pulse ratio for short time intervals, albeit a similar recovery to controls was inferred from time intervals ≥ 30 s. Although synaptic complexity underlying long lasting depolarizations (Carlson et al., 2000) limits defining the precise mechanism mediating short-term depression, the observation of a comparable paired pulse plasticity suggests the correct functional insertion of incipient synaptic contacts within pre-existing circuitry.

DISCUSSION

Taking advantage of the ability of *Xenopus* tadpoles to rewire neuronal networks after injury, the present work shows that recovery of basic olfactory-guided behavior is tightly coupled to the formation of synaptic contacts between newborn OSNs and the pre-existing olfactory bulb circuitry. The functional reconnection of rewired synapses is supported by the presence of well-defined active zones, as well as the ability to generate calcium transients and long lasting depolarizations in reponse to waterborne odorants. Formation of olfactory glomeruli requires weeks, is dictated by the postsynaptic environment but is not required to convey information. These results demonstrate that a reduced number of operative synapses, by being properly connected are capable to process information and set the basis of behavior.

The description of a close temporal coupling between formation and proper information processing in synaptic contacts established by OSNs provides a framework for understanding how intraglomerular connectivity is maintained during neuronal turnover (Cheetham & Belluscio, 2014; Mombaerts, 2006). As new OSNs appear in the olfactory epithelium, they send axons to the olfactory bulb. Upon leaving the nerve layer, axonal processes find their glomerulus and start to establish synapses. Growth of the axonal tuft is coordinated with the gradual increase in the number of active zones and the expansion of the cytoplasmic vesicle pool. Incipient OSN contacts show a high vesicle density in their active zones, thus suggesting the formation of a stable functional readily releasable pool (RRP). The constant presence of 100-150 synaptic vesicles·μm^{-2} in the cytoplasm supports that a vesicle reservoir permanently supplies active zones throughout development. This is a key difference to conventional synapses, which undergo a characteristic maturation of synaptic vesicle pools. Immature synapses typically display a readily releasable pool (RRP)/cytoplasmic pool ratio ~1, which shifts to ~0.3 within three weeks (Mozhayeva et al., 2002). Maturation is caused by the development of the cytoplasmic vesicle pool, while maintaining the size of the RRP constant.. The high number of vesicles that could be shared among neighboring synapses (Staras et al., 2010) within the tortuous presynaptic axons is presumably key for setting synaptic fidelity.

Contrary to the visual system or the cerebellum, axonal OSNs arbors do not display exuberant growth (Klenoff & Greer, 1998; Terni, López-Murcia, & Llobet, 2017). New synapses must be precisely inserted during normal neuronal turnover of intraglomerular connectivity. The net growth of axonal branches is thus associated to the establishment of novel synaptic contacts. Although the number of synaptic contacts varies with age (Hassenklöver & Manzini, 2013; Klenoff & Greer, 1998), the large amount of cytoplasmic vesicles distributed throughout the axonal arbor is likely available to any active zone. Considering the comparable organization among release sites throughout rewiring (Figs. 5 and 6), the main difference among all OSNs projecting to a single glomerulus would essentially be the number of contacts established. Older

neurons would likely display more complex presynaptic processes, containing more active zones than younger ones; however, the synaptic properties of any release site would be rather equivalent. This age-independent contribution of intraglomerular synapses established by OSNs provides an explanation for how constant neuronal turnover does not alter formation of odor maps.

Our behavioral test provided a binary response to odor detection. It allowed assigning a temporal window to detect the recovery of olfaction after injury, however, the test did not provide information about odor discrimination or sensitivity. The observation that small amplitude, long lasting depolarizations, could be evoked upon synapse formation suggests that intraglomerular circuitry is scaled-up during growth: as OSNs establish more synapses with M/T cells, gain is increased. The sensitivity to detect odors is likely enhanced by glomerular growth. But in terms of re-gaining the capacity for odor discrimination synaptic rewiring should probably require longer, waiting for the establishment of interglomerular connectivity (Aungst et al., 2003). The ability to discriminate odorants after injury is delayed upon the reacquisition of olfaction (Yee & Costanzo, 1995), which could be consistent with the rapid establishment of intraglomerular connectivity followed by the consolidation of interglomerular contacts. Our study uses nerve transection that affects to all OSNs and depicts an extreme situation of synaptic rewiring. Normal neuronal turnover causes the synchronous replacement of just few sensory neurons and, contrary to our experimental approach glomerular structure is maintained. The flow of information remains unaltered, thus allowing correct lateral information processing and providing a scaffold for the fast re-insertion of synapses.

ACKNOWLEDGEMENTS

We thank the National *Xenopus* Resource RRID:SCR_013731 (Woods Hole, MA). This work was supported by grants from El Ministerio de Economía y Competitividad (MINECO; SAF2015-63568-R) cofunded by the European Regional Development Fund (ERDF), Fundació

491 La Marató de TV3 (111530, to A.L. and P.G.), and by competitive research awards from the M.
492 G. F. Fuortes Memorial Fellowship, the Stephen W. Kuffler Fellowship Fund, the Laura and
493 Arthur Colwin Endowed Summer Research Fellowship Fund, the Fischbach Fellowship, and the
494 Great Generation Fund of the Marine Biological Laboratory, where a portion of this work was
495 conducted under the auspices of these awards.

REFERENCES

Arber, S., Han, B., Mendelsohn, M., Smith, M., Jessell, T. M., & Sockanathan, S. (1999). Requirement for the homeobox gene Hb9 in the consolidation of motor neuron identity. *Neuron, 23*(4), 659-674.

Aungst, J. L., Heyward, P. M., Puche, A. C., Karnup, S. V., Hayar, A., Szabo, G., & Shipley, M. T. (2003). Centre-surround inhibition among olfactory bulb glomeruli. *Nature, 426*(6967), 623-629. doi:10.1038/nature02185

Bressel, O. C., Khan, M., & Mombaerts, P. (2016). Linear correlation between the number of olfactory sensory neurons expressing a given mouse odorant receptor gene and the total volume of the corresponding glomeruli in the olfactory bulb. *J Comp Neurol, 524*(1), 199-209. doi:10.1002/cne.23835

Carlson, G. C., Shipley, M. T., & Keller, A. (2000). Long-lasting depolarizations in mitral cells of the rat olfactory bulb. *J Neurosci, 20*(5), 2011-2021.

Cheetham, C. E., & Belluscio, L. (2014). Neuroscience. An olfactory critical period. *Science, 344*(6180), 157-158. doi:10.1126/science.1253136

Cheetham, C. E., Park, U., & Belluscio, L. (2016). Rapid and continuous activity-dependent plasticity of olfactory sensory input. *Nat Commun, 7*, 10729. doi:10.1038/ncomms10729

Doucette, J. R., Kiernan, J. A., & Flumerfelt, B. A. (1983). The re-innervation of olfactory glomeruli following transection of primary olfactory axons in the central or peripheral nervous system. *J Anat, 137 (Pt 1)*, 1-19.

Flanagan-Steet, H., Fox, M. A., Meyer, D., & Sanes, J. R. (2005). Neuromuscular synapses can form in vivo by incorporation of initially aneural postsynaptic specializations. *Development, 132*(20), 4471-4481. doi:10.1242/dev.02044

Friedman, H. V., Bresler, T., Garner, C. C., & Ziv, N. E. (2000). Assembly of new individual excitatory synapses: time course and temporal order of synaptic molecule recruitment. *Neuron, 27*(1), 57-69. doi:S0896-6273(00)00009-X [pii]

Friedrich, R. W., & Korsching, S. I. (1997). Combinatorial and chemotopic odorant coding in the zebrafish olfactory bulb visualized by optical imaging. *Neuron, 18*(5), 737-752.

Gaudin, A., & Gascuel, J. (2005). 3D atlas describing the ontogenic evolution of the primary olfactory projections in the olfactory bulb of Xenopus laevis. *J Comp Neurol, 489*(4), 403-424. doi:10.1002/cne.20655

Gire, D. H., Franks, K. M., Zak, J. D., Tanaka, K. F., Whitesell, J. D., Mulligan, A. A., . . . Schoppa, N. E. (2012). Mitral cells in the olfactory bulb are mainly excited through a multistep signaling path. *J Neurosci, 32*(9), 2964-2975. doi:10.1523/JNEUROSCI.5580-11.2012

Hassenklöver, T., & Manzini, I. (2013). Olfactory wiring logic in amphibians challenges the basic assumptions of the unbranched axon concept. *J Neurosci, 33*(44), 17247-17252. doi:10.1523/JNEUROSCI.2755-13.2013

Hassenklöver, T., Pallesen, L. P., Schild, D., & Manzini, I. (2012). Amino acid- vs. peptide-odorants: responses of individual olfactory receptor neurons in an aquatic species. *PLoS One, 7*(12), e53097. doi:10.1371/journal.pone.0053097

Haws, M. E., Jaramillo, T. C., Espinosa, F., Widman, A. J., Stuber, G. D., Sparta, D. R., . . . Powell, C. M. (2014). PTEN knockdown alters dendritic spine/protrusion morphology, not density. *J Comp Neurol, 522*(5), 1171-1190. doi:10.1002/cne.23488

Herzog, C. D., & Otto, T. (2002). Administration of transforming growth factor-alpha enhances anatomical and behavioral recovery following olfactory nerve transection. *Neuroscience, 113*(3), 569-580.

Hinds, J. W., & Hinds, P. L. (1976). Synapse formation in the mouse olfactory bulb. II. Morphogenesis. *J Comp Neurol, 169*(1), 41-61. doi:10.1002/cne.901690104

Kasowski, H. J., Kim, H., & Greer, C. A. (1999). Compartmental organization of the olfactory bulb glomerulus. *J Comp Neurol, 407*(2), 261-274.

Klenoff, J. R., & Greer, C. A. (1998). Postnatal development of olfactory receptor cell axonal arbors. *J Comp Neurol, 390*(2), 256-267.

Lu, X. C., & Slotnick, B. M. (1998). Olfaction in rats with extensive lesions of the olfactory bulbs: implications for odor coding. *Neuroscience, 84*(3), 849-866.

Manzini, I., Brase, C., Chen, T. W., & Schild, D. (2007). Response profiles to amino acid odorants of olfactory glomeruli in larval Xenopus laevis. *J Physiol, 581*(Pt 2), 567-579. doi:jphysiol.2007.130518 [pii]

10.1113/jphysiol.2007.130518

Manzini, I., Heermann, S., Czesnik, D., Brase, C., Schild, D., & Rössler, W. (2007). Presynaptic protein distribution and odour mapping in glomeruli of the olfactory bulb of Xenopus laevis tadpoles. E*ur J Neurosci, 26(*4), 925-934. doi:EJN5731 [pii]

10.1111/j.1460-9568.2007.05731.x

Manzini, I., & Schild, D. (2004). Classes and narrowing selectivity of olfactory receptor neurons of Xenopus laevis tadpoles. J *Gen Physiol, 123(2*), 99-107. doi:jgp.200308970 [pii]

10.1085/jgp.200308970

Marsh-Armstrong, N., Huang, H., Berry, D. L., & Brown, D. D. (1999). Germ-line transmission of transgenes in Xenopus laevis. Pro*c Natl Acad Sci U S A, 96(25*), 14389-14393.

Meijering, E., Dzyubachyk, O., & Smal, I. (2012). Methods for cell and particle tracking. Met*hods Enzymol, 504, 1*83-200. doi:10.1016/B978-0-12-391857-4.00009-4

Mombaerts, P. (2006). Axonal wiring in the mouse olfactory system. Ann*u Rev Cell Dev Biol, 22,* 713-737. doi:10.1146/annurev.cellbio.21.012804.093915

Mozhayeva, M. G., Sara, Y., Liu, X., & Kavalali, E. T. (2002). Development of vesicle pools during maturation of hippocampal synapses. J N*eurosci, 22(3)*, 654-665. doi:22/3/654 [pii]

569 Nakano, T., Windrem, M., Zappavigna, V., & Goldman, S. A. (2005). Identification of a
570 conserved 125 base-pair Hb9 enhancer that specifies gene expression to spinal motor neurons.
571 Dev *Biol, 283(2)*, 474-485. doi:10.1016/j.ydbio.2005.04.017

572 Nezlin, L. P., Heermann, S., Schild, D., & Rössler, W. (2003). Organization of glomeruli in the
573 main olfactory bulb of Xenopus laevis tadpoles. J C*omp Neurol, 464(3)*, 257-268.
574 doi:10.1002/cne.10709

575 Nezlin, L. P., & Schild, D. (2000). Structure of the olfactory bulb in tadpoles of Xenopus laevis.
576 Cel*l Tissue Res, 302(1)*, 21-29.

577 Nussbaum-Krammer, C. I., Neto, M. F., Brielmann, R. M., Pedersen, J. S., & Morimoto, R. I.
578 (2015). Investigating the spreading and toxicity of prion-like proteins using the metazoan model
579 organism C. elegans. J V*is Exp(95*), 52321. doi:10.3791/52321

580 Rizzoli, S. O. (2014). Synaptic vesicle recycling: steps and principles. EMB*O J.*
581 *d*oi:10.1002/embj.201386357

582 Shepherd, G. M. (1972). Synaptic organization of the mammalian olfactory bulb. Phy*siol Rev,*
583 *52(4)*, 864-917.

584 Shepherd, G. M., Chen, W. R., & Greer, C. A. (2004). The *Synaptic Organization of the Brain*
585 *(G*. M. Shepherd Ed.): Oxford University Press.

586 Singleton, C. D., & Casagrande, V. A. (1996). A reliable and sensitive method for fluorescent
587 photoconversion. J N*eurosci Methods, 64(1)*, 47-54.

588 Staras, K., Branco, T., Burden, J. J., Pozo, K., Darcy, K., Marra, V., . . . Goda, Y. (2010). A
589 vesicle superpool spans multiple presynaptic terminals in hippocampal neurons. Neu*ron, 66(1)*,
590 37-44. doi:10.1016/j.neuron.2010.03.020

591 Stout, R. P., & Graziadei, P. P. (1980). Influence of the olfactory placode on the development of
592 the brain in Xenopus laevis (Daudin). I. Axonal growth and connections of the transplanted
593 olfactory placode. Neu*roscience, 5(12*), 2175-2186.

594 Terni, B., López-Murcia, F. J., & Llobet, A. (2017). Role of neuron-glia interactions in
595 developmental synapse elimination. Bra*in Res Bull, 129,* 74-81.
596 doi:10.1016/j.brainresbull.2016.08.017

597 Treloar, H. B., Feinstein, P., Mombaerts, P., & Greer, C. A. (2002). Specificity of glomerular
598 targeting by olfactory sensory axons. J N*eurosci, 22(7)*, 2469-2477. doi:20026239

599 Waites, C. L., Craig, A. M., & Garner, C. C. (2005). Mechanisms of vertebrate synaptogenesis.
600 Ann*u Rev Neurosci, 28,* 251-274. doi:10.1146/annurev.neuro.27.070203.144336

601 Yee, K. K., & Costanzo, R. M. (1995). Restoration of olfactory mediated behavior after olfactory
602 bulb deafferentation. Phy*siol Behav, 58(5)*, 959-968.

603 Yoshino, J., & Tochinai, S. (2006). Functional regeneration of the olfactory bulb requires
604 reconnection to the olfactory nerve in Xenopus larvae. Dev *Growth Differ, 48(1)*, 15-24.
605 doi:DGD [pii]

606 10.1111/j.1440-169X.2006.00840.x

607 Zou, D. J., Chesler, A., & Firestein, S. (2009). How the olfactory bulb got its glomeruli: a just so
608 story? Nat *Rev Neurosci, 10(8),* 611-618. doi:10.1038/nrn2666

609

Figure 1. Examples of tadpoles showing recovery of olfactory guided behavior upon transection of olfactory nerves. a) Tracking of tadpole movements. The arrow indicates the position of the tube delivering a 160 μM solution of five amino acids (methionine, leucine, histidine, arginine, lysine). Tadpole positions before and after amino acid application are indicated in green and orange, respectively. Movements during odorant exposure are shown in a temporal gray scale. **b)** Measurement of the euclidean distance of the tadpole head to the solution inlet as a function of time for the animal shown in A). Colors indicate position before, during and after application of amino acids, as in A). Bar shows the increase in [aas]. **c, d)** Same as B) for tadpoles with both olfactory nerves transectioned. Plots correspond to individual examples of behavioral assays 1 day after cut (D1, blue) and 4 days after cut (D4, red).

Figure 2. Emergence of olfactory guided behavior after olfactory nerve transection. Average euclidean distances expressed as mean±s.e.m (line±shadowed area) plotted as a function of time. Tadpole positions were grouped before exposure to waterborne odorants by baseline subtracting distances at the onset of stimulation. The increases and decreases in tadpole distance to the odor source are associated to positive or negative changes in the euclidean distance, respectively . **a)** Tadpoles did not react to the application of water. Control (n=51), 1 day after transection (D1,n=39) and 4 days after transection (D4, n=54). **b-d)** Olfactory guided response in tadpoles exposed to the amino acid mixture, control (n=63), D1 (n=55) and D4 (n=63). Notice the linear decrease in the euclidean distance during odor application in control and D4 groups compared to D1 tadpoles.

Figure 3. Time course of olfactory nerve reformation after transection. A single olfactory nerve of tubb2-GFP *X. laevis* or NBT-GFP tadpoles was cut (arrow), leaving the contralateral one as control. **a)** Image of a tubb2-GFP *X. laevis* tadpoles immediately after (D0) transection of a single olfactory nerve (arrow). Both olfactory placodes were injected with DiI after nerve cut to validate transection by measuring the spread of the dye (red line) **b)** Plot of DiI fluorescence intensity normalized to the placode level along sectioned nerves (n=5). Dye diffused for 24 h (D1). **c)** Tadpoles with olfactory pathways stained by DiI were fixed and sectioned. Notice the lack of fluorescence in the olfactory bulb innervated by the cut olfactory nerve (asterisk). The dotted yellow line indicates the separation between the mitral cell layer (MCL) and the glomerular layer (GL). The position of the olfactory nerve (ON) is also indicated. **d)** Images show the reformation of the olfactory nerve in four different tubb2-GFP *X. laevis* tadpoles at the indicated times after surgery. **e)** Time-course of olfactory nerve reformation. Plot shows the percentage of successful reconnection to the olfactory bulb (up, % Reform.) and the relative increase in olfactory nerve (O.N.) width as a function of time (down).

Figure 4. Synaptic rewiring and formation of glomerular connectivity after olfactory nerve transection. a, b) Control and rewired olfactory bulbs from two *X. laevis* tubb2-GFP tadpoles subjected to unilateral transection of the olfactory nerve, 8 and 15 days after cut, respectively. The asterisk indicates the ipsilateral bulb to the sectioned nerve. Immunohistochemistry for GFP and synaptophysin revealed the location of neuronal processes (green) and synapses (red), respectively. Nuclei were stained with draq-5 (blue). **c)** Change of glomerular perimeter during normal development (black) and upon nerve reformation (red). **d, e)** Images of the olfactory bulb of living zHB9-GFP *X. tropicalis* tadpoles embedded in agarose 4 and 8 days after unilateral nerve transection. The asterisk indicates the ipsilateral bulb to the injured nerve. Control bulb shows three distinct glomerular structures (L, M1 and M2). A minimal labeling of the L glomerulus is observed in the rewired bulb 8 days after cut. **f)** Histological section of the lateral glomerulus from a control bulb. Arrowheads indicate axonal varicosities presumably associated to synaptic contacts. **g)** Same as f), but for a bulb rewired 8 days after olfactory nerve transection **h)** Relationship between the total volume of glomerular structures identified in a given olfactory

bulb and the number of GFP positive cell bodies found in the corresponding ipsilateral placode. A linear fit through binned data provided a slope of 874 μm^3.

Figure 5. Morphological appearence of rewired synaptic contacts. a) Low magnification electron microscopy image of a control glomerulus (dotted line). **b, c)** Higher magnification images of synapses established by olfactory sensory neurons (dark cytoplasm) within a control glomerulus (arrows in A). **d)** Precursors of glomerular structures are evident 4 days after injury (dotted line). **e, f)** Profile of two synaptic contacts reformed 4 days after transection. **g-i)** Appearance of glomerular structures (dotted line) and synaptic contacts 6 days after injury. **j-l**) Olfactory glomeruli (dotted line) and synapses established by olfactory sensory neurons 15 days after transection are comparable to controls.

Figure 6. Properties of olfactory sensory neuron terminals during rewiring of olfactory glomeruli. **a)** Average length and number of vesicles attached to an active zone (<100 nm, single section) at the indicated times after injury. Control is shown at "day 0". **b)** Distribution of cytoplasmic vesicles as a function of rewiring time. Asterisk indicates statistical difference (One-way ANOVA, $p<0.01$).

Figure 7. Olfactory nerves rerouted to the hindbrain establish an aberrant connectivity. a) Images of *X. laevis* tubb2-GFP tadpoles. Rerouting of the sectioned olfactory nerve (asterisk) to the hindbrain. Olfactory pathways are revealed by local application of DiI-CM to placodes. **b)** Images of a single tadpole 5, 13 and 16 days after cut show that rerouted nerve (yellow arrows) is stable. The location of the optic nerve is indicated (green arrows). **c)** Tadpoles showing aberrant nerves were fixed and processed for histology to reveal DiI labeled processes at the level of the hindbrain (arrows). **d-f)** DiI was photoconverted for visualization by electron microscopy. This method allows observing the complex network of OSN axons (arrows) within glomeruli. **g-i)** Photoconverted axons at the level of the hindbrain do not form glomeruli (g) but establish putative synaptic contacts (h and i).

Figure 8. Functional responses of incipient glomerular synapses. a, b) Transmitted light images of the control (a) and rewired (b) bulbs from two different tadpoles showing OSN terminals labeled with calcium green dextran. **c, d)** Corresponding $\Delta F/F$ images obtained during 0.5 s application of a 200 μM amino acid mixture to the ipsilateral olfactory placode. **e)** Time-course of calcium transients evoked by exposure to odorants. Grey traces indicate responses from glomerular regions. The average transient is indicated in black (control) and red (4 days after cut, D4).

Figure 9. Incipient synapses evoke long lasting depolarizations in the glomerular layer. a,b) Long lasting depolarizations recorded in the glomerular layer as changes in the local field potential (LFP). Grey traces indicate single responses upon 0.1 s application of the 200 μM amino acid solution. The average response (mean±s.e.m.) is shown in black (controls) and red (4 days after cut, D4). **c)** Individual (open circles) and average (dots, mean±s.e.m.) amplitude of LFP responses in control (n=64) and D4 tadpoles (n=25). Asterisk indicates statistical difference (Student's t-test, $p<0.001$). **d)** Paired-pulse depression observed upon application of the 200 μM amino acid solution in a tadpole subject to unilateral sectioning of an olfactory nerve. Recordings show single responses obtained at the indicated time intervals for control (black) and rewired (D4, red) bulbs. **e)** Recovery of paired-pulse depression for control (black) and rewired (D4, red) bulbs. Dots indicate mean±s.e.m. (n=6), fitted with a single exponential function (τ=18 s).

Figure 1

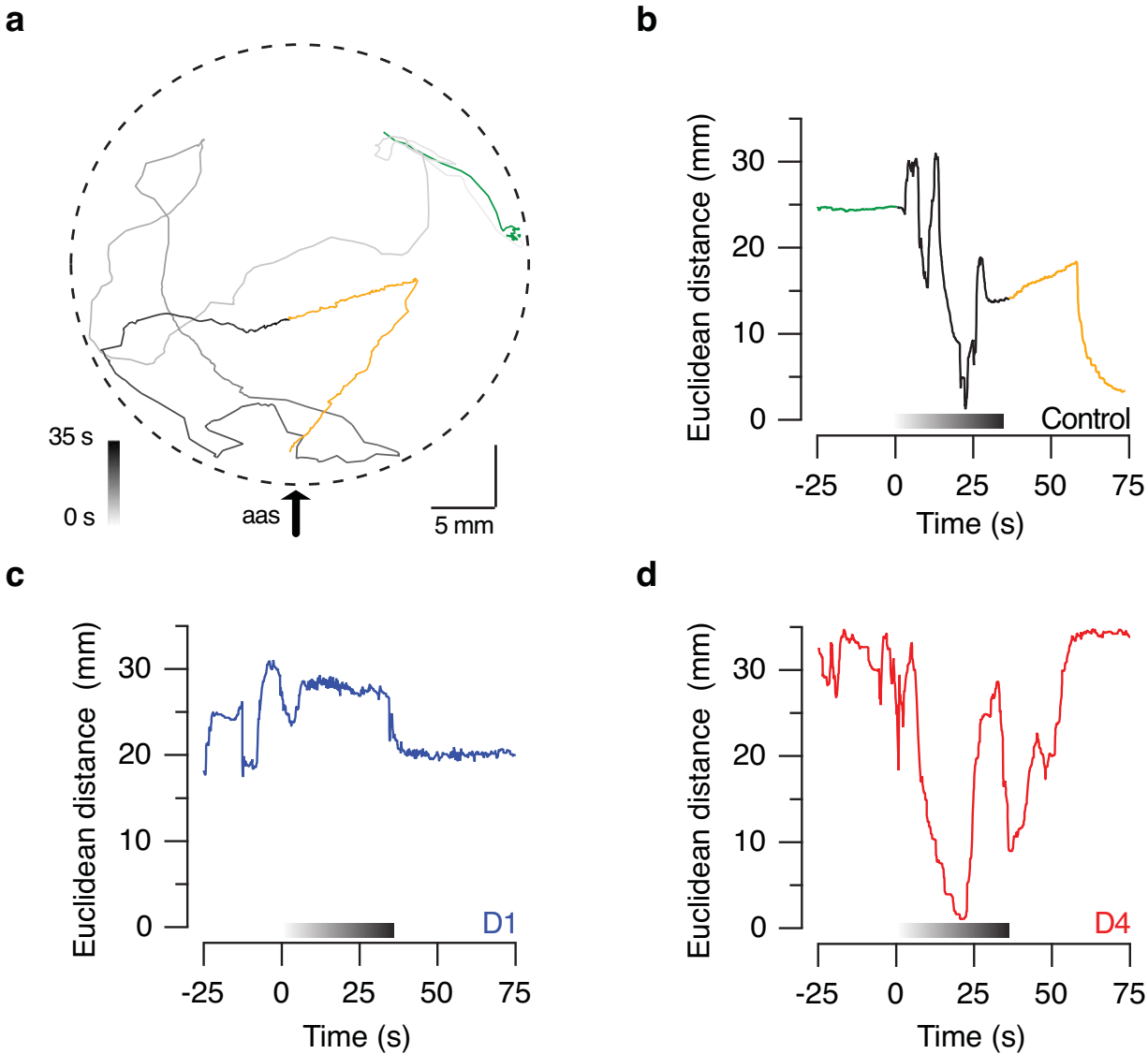
a
35 s
0 s
aas
5 mm
b
Euclidean distance (mm)
30
20
10
0
Control
-25
0
25
50
75
Time (s)
c
Euclidean distance (mm)
30
20
10
0
D1
-25
0
25
50
75
Time (s)
d
Euclidean distance (mm)
30
20
10
0
D4
-25
0
25
50
75
Time (s)

Figure 2

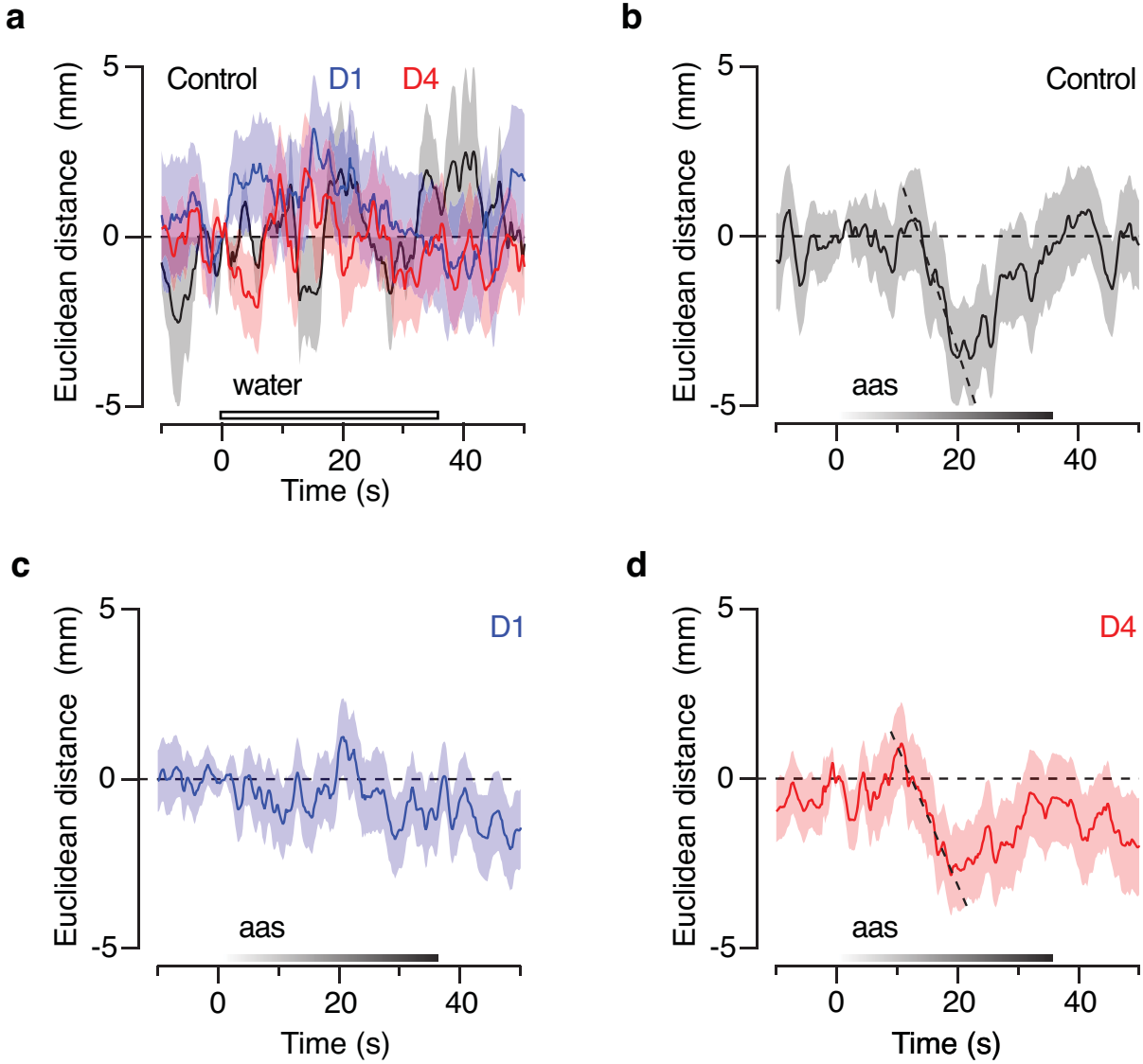
a
Control
D1
D4
Euclidean distance (mm)
5
0
-5
water
0
20
40
Time (s)
b
Control
aas
c
D1
d
D4

Figure 3

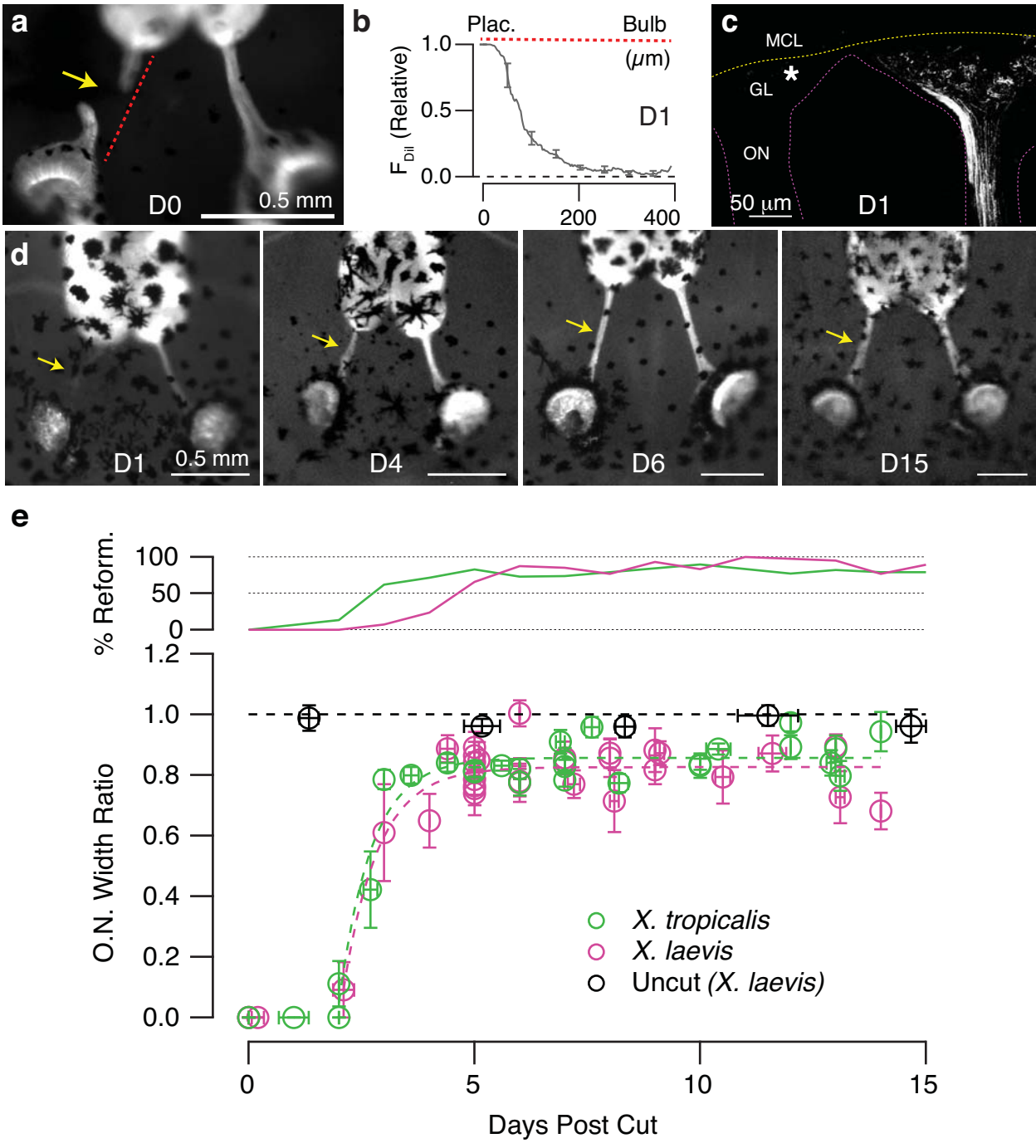
a
D0
0.5 mm
b
Plac.
Bulb
(μm)
D1
F_Dil (Relative)
1.0
0.5
0.0
0
200
400
c
MCL
GL
ON
50 μm
D1
d
D1
0.5 mm
D4
D6
D15
e
% Reform.
100
50
0
O.N. Width Ratio
1.2
1.0
0.8
0.6
0.4
0.2
0.0
X. tropicalis
X. laevis
Uncut (X. laevis)
0
5
10
15
Days Post Cut

Figure 4

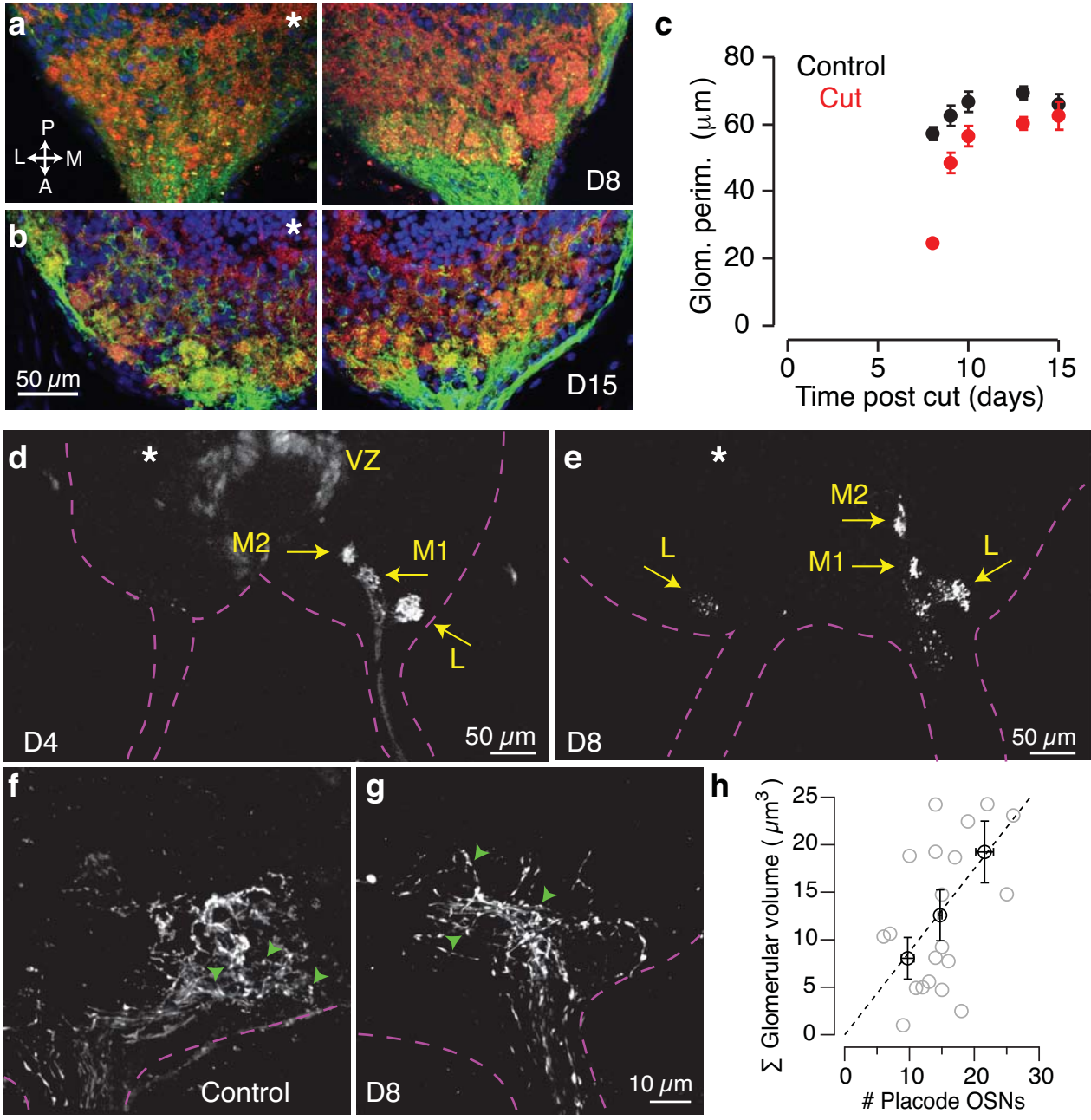
a
*
P
L
M
A
D8
b
*
50 μm
D15
c
Control
Cut
Glom. perim. (μm)
80
60
40
20
0
0
5
10
15
Time post cut (days)
d
*
VZ
M2
M1
L
D4
50 μm
e
*
M2
M1
L
L
D8
50 μm
f
Control
g
D8
10 μm
h
Σ Glomerular volume (μm3)
25
20
15
10
5
0
0
10
20
30
Placode OSNs

Figure 5

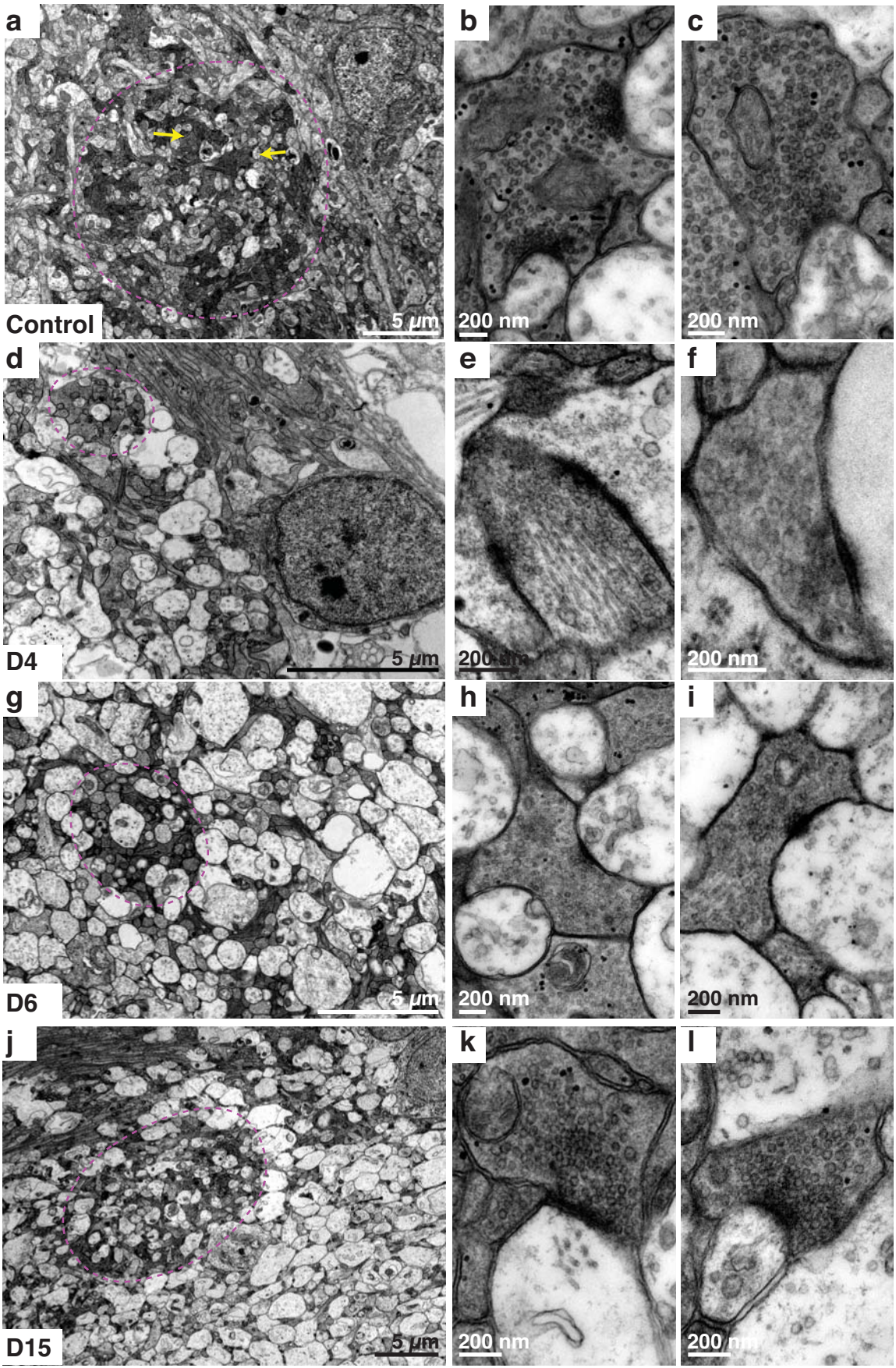
a
b
c
Control
5 μm
200 nm
200 nm
d
e
f
D4
5 μm
200 nm
200 nm
g
h
i
D6
5 μm
200 nm
200 nm
j
k
l
D15
5 μm
200 nm
200 nm

Figure 6

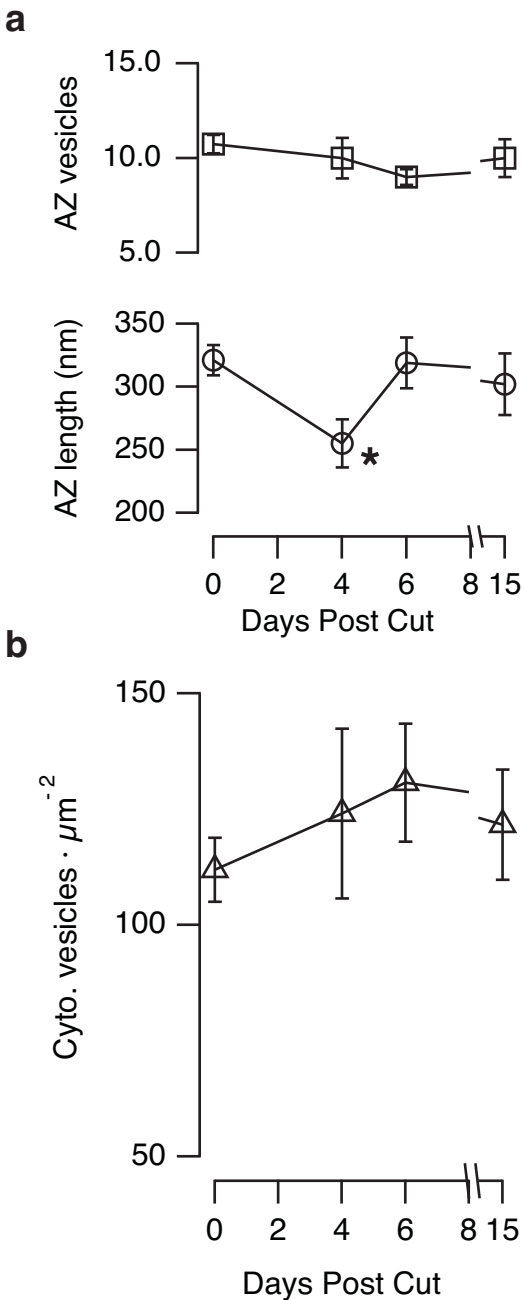
a
15.0
10.0
5.0
AZ vesicles
350
300
250
200
AZ length (nm)
*
0
2
4
6
8
15
Days Post Cut
b
150
100
50
Cyto. vesicles · µm-2
0
2
4
6
8
15
Days Post Cut

Figure 7

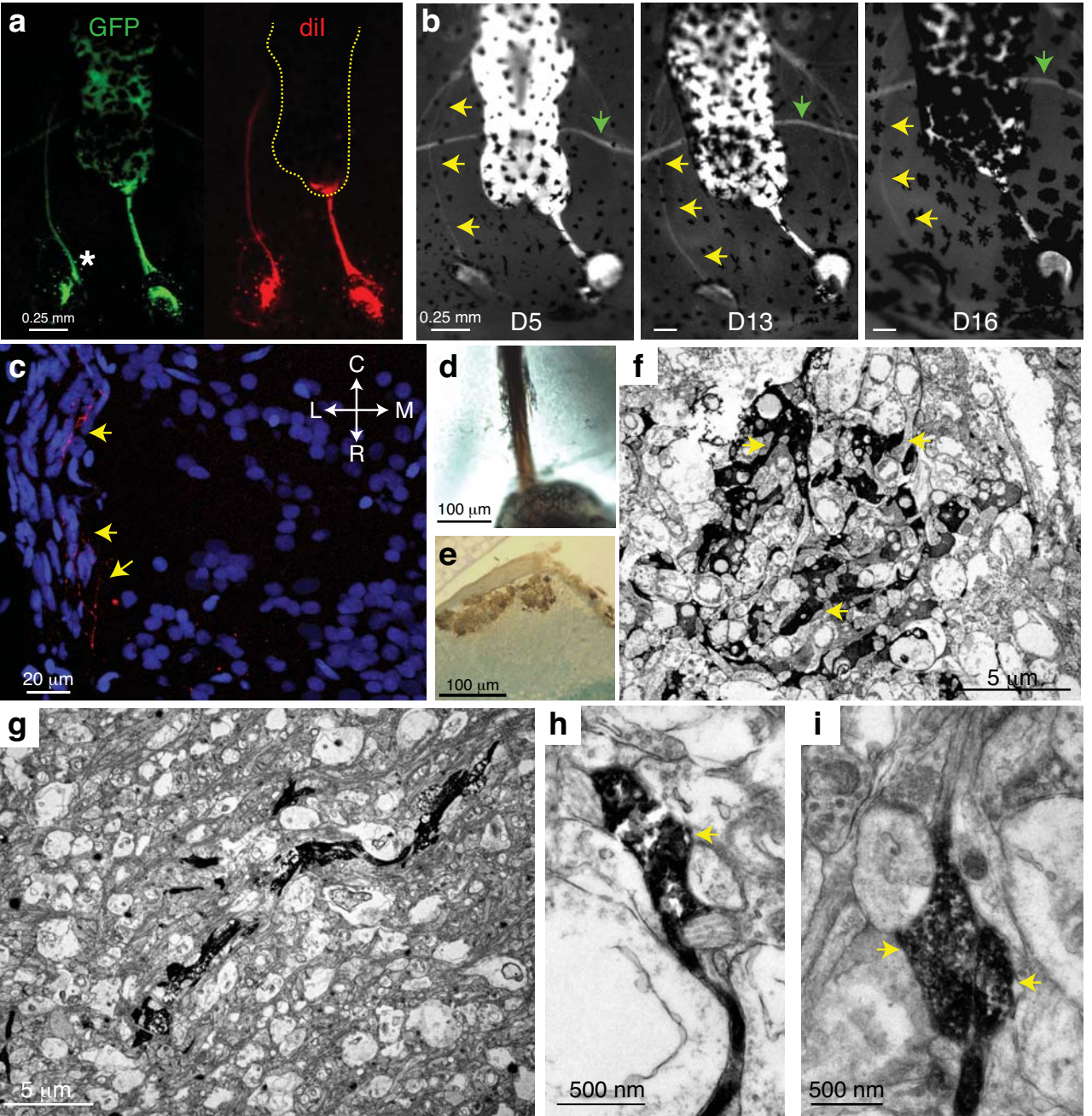
a
GFP
dil
*
0.25 mm
b
0.25 mm
D5
D13
D16
c
C
L
M
R
20 µm
d
100 µm
e
100 µm
f
5 µm
g
5 µm
h
500 nm
i
500 nm

Figure 8

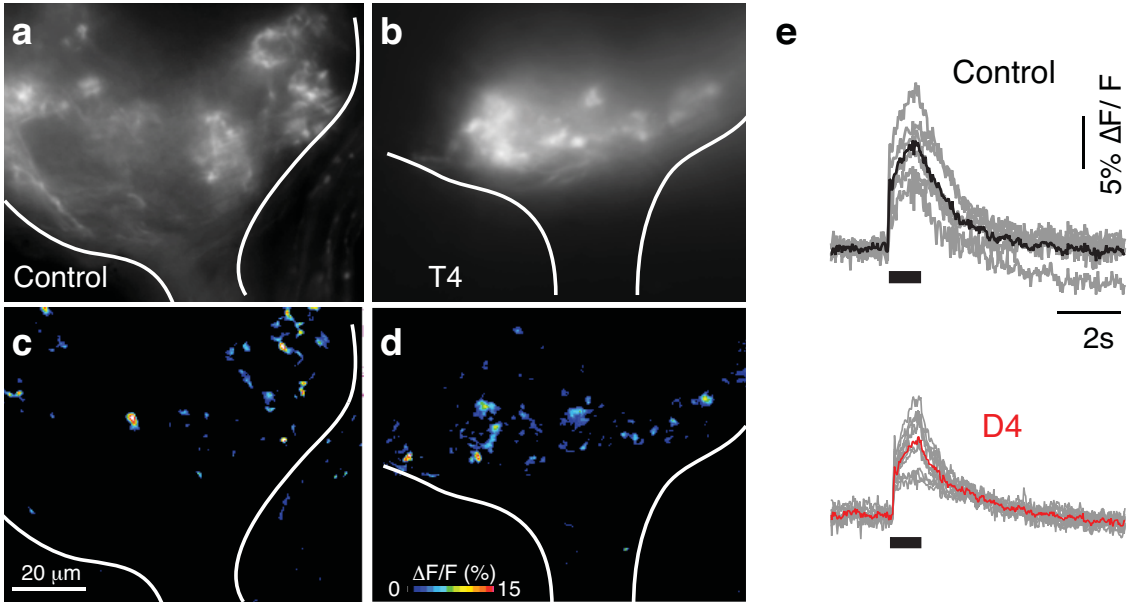

Figure 9

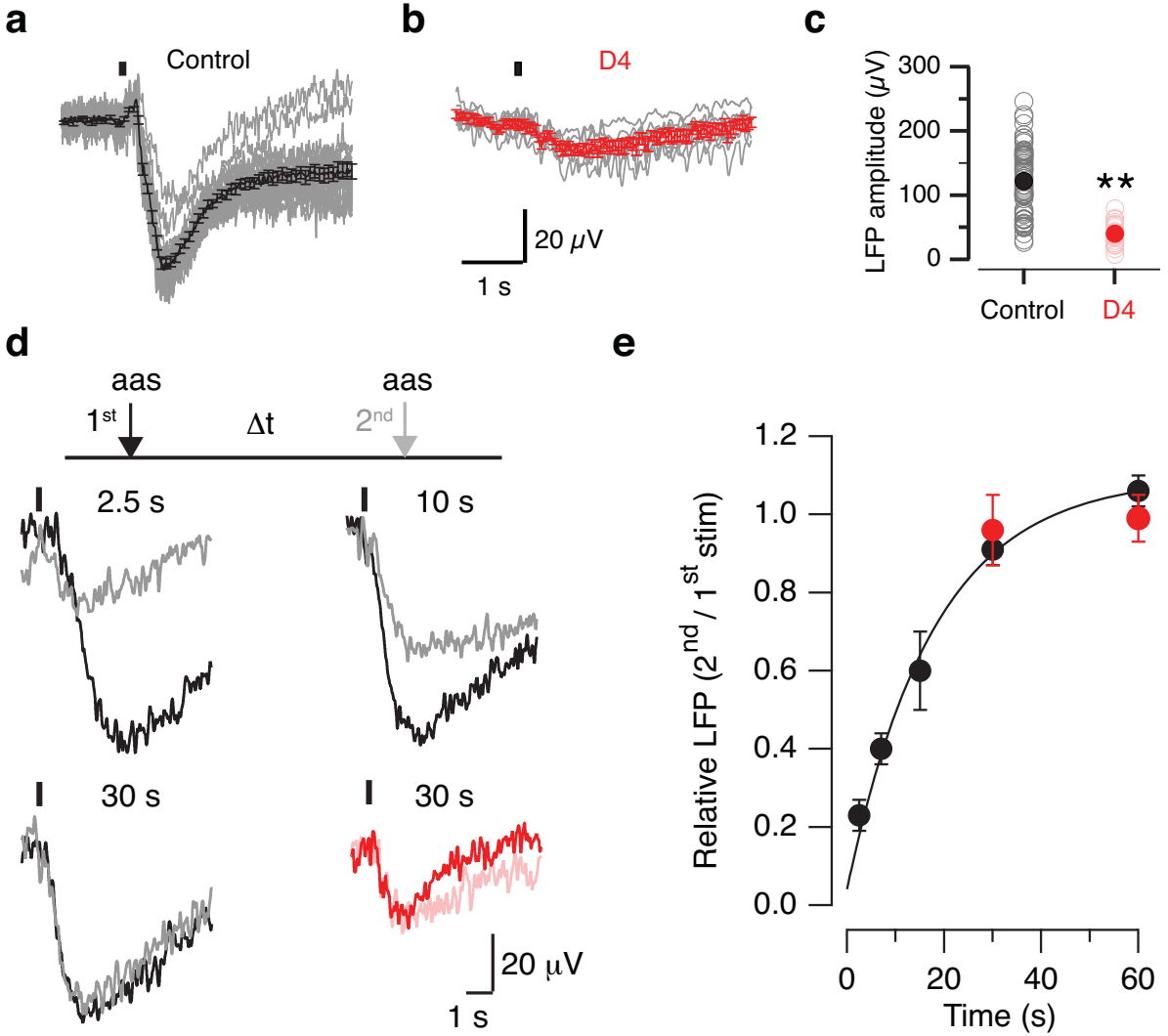
a
Control
b
D4
20 μV
1 s
c
LFP amplitude (μV)
300
200
100
0
**
Control
D4
d
aas
1st
Δt
2nd
aas
2.5 s
10 s
30 s
30 s
20 μV
1 s
e
Relative LFP (2nd / 1st stim)
1.2
1.0
0.8
0.6
0.4
0.2
0.0
0
20
40
60
Time (s)